Supplementary materials to

Intra-regional transport of black carbon between North China Plain and Central China during winter haze episodes

Huang Zheng[1,2], Shaofei Kong[1], Fangqi Wu[1], Yi Chen[1], Zhenzhen Niu[1], Shurui Zheng[1], Guowei Yang[1], Liquan Yao[2], Qin Yan[1,2], Jian Wu[1,2], Mingming Zheng[2,3], Nan Chen[3], Ke Xu[3], Yingying Yan[1], Dantong Liu[4], Delong Zhao[5], Tianliang Zhao[6], Yongqing Bai[7], Shuanglin Li[1], and Shihua Qi[2]

[1]Department of Atmospheric Science, School of Environmental Sciences, China University of Geosciences, Wuhan, 430074, China

[2]Department of Environmental Science and Technology, School of Environmental Sciences, China University of Geosciences, Wuhan, 430074, China

[3]Hubei Provincial Environmental Monitoring Centre, Wuhan, 430072, China

[4]School of Earth, Atmospheric & Environmental Sciences, University of Manchester, M139PL, UK

[5]Beijing Weather Modification Office, Beijing, 100089, China

[6]School of Atmospheric Physics, Nanjing University of Information Science and Technology, Nanjing, 210044, China

[7]Hubei Key Laboratory for Heavy Rain Monitoring and Warning Research, Institute of Heavy Rain, China Meteorological Administration, Wuhan, 430205, China

Correspondence to: Shaofei Kong (kongshaofei@cug.edu.cn)

Text S1 Description of CWT

To distinguish the pollution levels of different potential regions, a concentration-weighted-trajectory (CWT) model was employed in this study. The CWT was calculated according to:

$$C_{\mathrm{ij}} = \frac{1}{\sum_{l=1}^{M} \tau_{ijl}} \sum_{l=1}^{N} c_l \tau_{ijl} \tag{1}$$

where C_{ij} represents the average weight concentrations in the grid cell (i, j); C_l is the measured BC concentration observed on the arrival of trajectory l; τ_{ijl} is the number of trajectory end points in the grid cell (i, j) associated with the C_l sample.

In order to consider only air parcels with good representativeness, a weighing function was added to the calculation to down weight cells associated with low values of n. The default weighting function was used as below:

$$W = \begin{cases} 1.00 & for \log(n+1) \geq 0.85 * max_{\log(n+1)} \\ 0.725 & for\ 0.60 * max_{\log(n+1)} > \log(n+1) \geq 0.85 * max_{\log(n+1)} \\ 0.475 & for\ 0.35 * max_{\log(n+1)} > \log(n+1) \geq 0.60 * max_{\log(n+1)} \\ 0.175 & for \log(n+1) < 0.35 * max_{\log(n+1)} \end{cases} \tag{2}$$

Table S1 Reported BC levels in China and around the world.

Station	Site type	Location (°N), (°E)	Inlet	Instrument	Sampling period	BC (μg m^{-3})	References
Hongan	Rural	31.24, 114.58	$PM_{2.5}$	AE33	2018.01	5.54 ± 2.59	This study
Luohe	Suburban	33.57, 114.05	$PM_{2.5}$	AE33	2018.01	8.48 ± 4.83	
Suixian	Rural	31.88, 113.28	—	AE51	2018.01	4.47 ± 2.90	
Wuhan	Urban	30.53, 114.39	$PM_{2.5}$	AE31	2018.01	3.91 ± 1.86	
Xiangyang	Suburban	32.02, 112.17	—	AE51	2018.01	7.35 ± 3.45	
YRD							
Nanjing	Urban	32.05, 118.78			2012 Annual	4.16 ± 2.63	(Zhuang et al., 2014)
Shanghai	Urban	31.23,121.53		AE31	2007.04–2010.03	3.83	(Wang et al., 2014a)
Jiaxin	Suburban	30.80, 120.8		SP2	2010.12	7.1	(Huang et al., 2013)
PRD							
Maofeishan	Rural	23.33, 113.48	PM_{10}	AE31	2008.12–2009.01	2.88	(Wu et al., 2013)
Nancuan	Suburban	23.00, 113,35	PM_{10}	AE31	2008.12–2009.01	7.68	
Panyu (PY)	Urban	22.93, 113.32	PM_{10}	AE31	2008.12–2009.01	20.21	
Dongguan	Suburban	22.97, 113.73	PM_{10}	AE31	2008.12–2009.01	10.11	
Xinken	Rural	22.71, 113.55	PM_{10}	AE31	2008.12–2009.01	12.61	
Hong Kong	Rural-costal	22.22, 114.25	$PM_{2.5}$	AE31	2012.02–2015.02	1	(Wang et al., 2017)
Shenzhen	Urban	22.60, 113.97		SP2	2010.01–02	4.1 ± 3.8	(Huang et al., 2012)
Shenzhen	Rural	22.65, 114.53			2009.11–12	2.6 ± 1.0	
NCP							
Beijing	Suburban	40.65, 117.12	—	AE31	2003.04–2005.01	2.12 ± 1.62	(Yan et al., 2008)
Beijing	Urban	39.93, 116.30	$PM_{2.5}$	AE31	2010.01–2014.12	3.67	(Liu et al., 2016)
Beijing	Urban	39.97, 116.37		SP2	2013.01	5.5	(Wu et al., 2016)
Xianghe	Rural	39.90, 116.96	PM_{10}	AE31	2013.04–2015.03	5	(Ran et al., 2016)
Beijing	Urban-rural	40.04, 116.41	$PM_{2.5}$	AE31	2014	4.4 ± 3.7	(Ji et al., 2017)
Beijing	Urban	39.98, 116.30	NP	AE33	2015.12–2016.02	5.31 ± 6.26	(Liu et al., 2018)
Tibetan							
Lulang	Remote area	29.46, 94.44		SP2	2015.09–10	0.31 ± 0.55	(Wang et al., 2018)
Qinghai Lake	Remote area	36.98, 99.88		SP2	2012.11.16–27	0.16 ± 0.19	(Wang et al., 2015)
Nam Co	Remote area	30.77, 90.99	$PM_{1.0}$	TOR	2012.09–12	0.09	(Wan et al., 2015)
Ranwu	Remote area	29.32, 96.96	NP	AE31	2012.11–2013.02	0.41	(Wang et al., 2016)
Beiluhe	Remote area	34.85, 92.94	NP	AE31	2012.11–2013.02	0.2	
Muztagh Ata	Remote area	38.28, 75.02	NP	AE16	2009.09	0.16 ±0.19	(Zhu et al., 2016)
National wide							
Chengdu	Urban	30.65, 104.04	PM_{10}	TOR	2006–07 Annual	10.8 ± 5.52	(Zhang et al., 2012)
Dalian	Urban	38.90, 121.63	PM_{10}	TOR	2006–07 Annual	5.28 ± 2.53	
Dunhuang	Rural	40.15, 94.68	PM_{10}	TOR	2006–07 Annual	4.09 ± 2.33	
Gaolanshan	Rural	36.00, 105.85	PM_{10}	TOR	2006–07 Annual	3.79 ± 2.01	
Gucheng	Rural	39.13, 115.8	PM_{10}	TOR	2006–07 Annual	10.6 ± 4.60	
Jinsha	Rural	39.63, 114.2	PM_{10}	TOR	2006–07 Annual	2.98 ± 1.21	
Lhasa	Urban	29.67, 91.13	PM_{10}	TOR	2006–07 Annual	3.87 ± 2.20	
LinAn	Rural	31.30, 119.73	PM_{10}	TOR	2006–07 Annual	4.24 ± 1.89	
Longfengshan	Rural	44.73, 127.60	PM_{10}	TOR	2006–07 Annual	2.25 ± 1.04	

Nanning	Urban	22.82, 108.35	PM_{10}	TOR	2006–07 Annual	3.84 ± 1.79	
Panyu	Urban	22.93, 113.32	PM_{10}	TOR	2006–07 Annual	7.54 ± 3.57	
Taiyangshan	Rural	29.17, 111.71	PM_{10}	TOR	2006–07 Annual	2.61 ± 1.15	
Zhengzhou	Urban	34.78, 113.68	PM_{10}	TOR	2006–07 Annual	9.43 ± 3.50	
Xi'an	Urban	34.43, 108.97	PM_{10}	TOR	2006–07 Annual	12.1 ± 4.62	
Xi'an	Urban	34.22, 109.00	PM_{10}	SP2	2012.12–2013.01	8.8 ± 3.7	(Wang et al., 2014b)
Lanzhou	Rural	35.57, 104.08	$PM_{2.5}$	AE31	2007.01–2009.08	1.57	(Zhang et al., 2011)
Shenyang	Urban	41.77, 123.50	NP	AE31	2008.03–2009.02	6.14	(Wang et al., 2011)
Dalian	Urban	38.90, 121.63	NP	AE31	2008.03–2009.02	3.18	
Anshan	Urban	41.08, 123.00	NP	AE31	2008.03–2009.02	5.3	
Fushun	Urban	41.88, 123.95	NP	AE31	2008.03–2009.02	4.16	
Benxi	Urban	41.32, 123.78	NP	AE31	2008.03–2009.02	6.78	
Changchun	Urban	43.90, 125.22	NP	AE31	2007.10–2008.01	15.6	(Gao et al., 2009)
Worldwide							
Finland							
Hyytiälä,	Forest		PM_{10}	AE31	2004.12–2008.12	0.32 ± 0.34	(Hyvärinen et al., 2011)
Puijo	Finland		$PM_{2.5}$	MAAP	2006.08–2008.12	0.23 ± 0.27	
Utö			$PM_{2.5}$	AE31	2007.01–2008.12	0.25 ± 0.33	
Virolahti			$PM_{2.5}$	AE31	2006.08–2008.12	0.42 ± 0.45	
Pallastunturi			PM_{10}	MAAP	2007.09–2008.12	0.06 ± 0.13	
Ontario							
HWY401	Near road	43.71, 79.54	$PM_{2.5}$	AE33	2015.06–2016.05	1.74	(Healy et al., 2017)
Etobicoke	Near road	43.61, 79.52	$PM_{2.5}$	AE33	2015.06−2016.05	0.95	
College St. G	Near road	43.65, 79.39	$PM_{2.5}$	AE33	2015.06−2016.05	0.84	
College St. R	Near road	43.65, 79.39	$PM_{2.5}$	AE33	2015.06−2016.05	0.59	
Scarborough	Near road	43.74. 9.27	$PM_{2.5}$	AE22	2015.06−2016.05	0.69	
Hamilton DTN	Near road	43.25, 79.86	$PM_{2.5}$	AE22	2015.06−2016.05	0.61	
Windsor DTN	Near road	42.31, 83.04	$PM_{2.5}$	AE22	2015.06−2016.05	0.55	
Windsor W	Residential	42.29, 83.07	$PM_{2.5}$	AE33	2015.06−2016.05	0.72	
Hanlan's Point	Background	43.61, 79.38	$PM_{2.5}$	AE33	2015.06−2016.05	0.51	
France							(Petit et al., 2017)
SIRTA	Semi-urban	48.71, 2.15		AE33		0.8	
Metz	Urban	49.11, 6.22		AE33		2.3	
Lyon	Urban	45.76, 4.85		AE33		1.7	
South Africa							(Chiloane et al., 2017)
Enlandsfontein	Top of hill	26.25 (s), 29.42		MAAP	2009.01−2011.05	0.8	
Marikana	Village	25.70 (s), 27.38		MAAP	2008.01−1010.05	1.2	
Amersfoort		27.07 (s), 29.87		MAAP	2010.01−2012.05	1.1	

TOR: Thermal/optical reflectance carbon analyzer;

SP2: single particle soot photometer;

MAAP: multi-angle absorption photometer;

Anthalometer, Magee Scientific, Mode

Table S2 Reported absorption coefficients of BC in China

Stations	Locations (°N), (°E)	Instrument	Sampling period	σ_{ap} (λ nm)	References
Hongan	31.24, 114.58	AE33	2018.01	86.0 (550)	This study
Luohe	33.57, 114.05	AE33	2018.01	132 (550)	
Wuhan	30.53, 114.39	AE31	2018.01	60.6 (550)	
YRD					
Nanjing	32.10, 119.90	AE31	2013.06−2015.05	26.1 (520)	(Shen et al., 2017)
	32.20, 118.70	PASS	2011.03−04	28.1 (532)	(Yu et al., 2016)
	32.05, 118.78	AE31	2014.03−2016.02	29.6 (520)	(Zhuang et al., 2017)
Shanghai	31.30, 121.48	AE31	2010.12−2011.03	66 (532)	(Xu et al., 2012)
	31.30, 121.48	AE31	2010.12−2012.10	38 (532)	(Cheng et al., 2015)
	40.04 N, 116.41	AE31	2014	38.7 (880)	(Ji et al., 2017)
Shouxian	32.56, 116.78	PSAP	2008.05−12	29.4 (550)	(Fan et al., 2010)
Lin'an	30.28, 119.75	PSAP	1999.10−12	23 (565)	(Xu et al., 2002)
PRD					
Guangzhou	23.00, 113.35		2004−2007	82 (532)	(Wu et al., 2009)
	23.92, 113.12		2006.07	42.5 (532)	(Garland et al., 2008)
Hong Kong	22.22, 114.25	AE31	2012−2015	8.30 (550)	(Wang et al., 2017b)
Panyu	23.00, 113.35	AE31	2014.02−03	45.7 (550)	(Tan et al., 2016)
Xinken	22.60, 113.60	MAAP	2004.10−11	37 (550)	(Cheng et al., 2008)
NCP					
Beijing	39.85, 116.52	PAS	2006.08	51.8 (532)	(Garland et al., 2009)
	39.98, 116.32	AE16	2005.01−2006.12	56 (525)	(He et al., 2009)
Tongyu	44.56, 122.92	AE31	2010.03	7.61 (520)	(Wu, 2012)
Wuqing	39.38, 117.02	MAAP	2009.03−05	19.1 (550)	(Ma et al., 2011)
Xianghe	39.75, 116.96	PSAP	2005.05	65.0 (550)	(Li et al., 2007)
Tibetan					
Lhasa	29.60, 91.10	AE33	2015.09−11	53 (370)	(Zhu et al., 2017)
Lulang	29.76, 94.73			15 (370)	
Qinghai Lake	36.98, 99.88	SP2	2012.11.16–27	2.1	(Wang et al., 2015)
National wide					
Chengdu	30.62, 104.07	AE31	2015.01−02	60.2	(Wang et al., 2017a)
Chongqin	29.62, 106.50		2015.01−02	66.6	
Xiamen	24.60, 118.05	PAX	2013.11−2014.01	22.4	(Deng et al., 2016)
Xi'an	34.23, 108.88	PAX	2012.8−10	31 (532)	(Zhu et al., 2015)
Jinan	36.67, 117.05	AE21	2013.12−2014.2	63 (532)	(Yan et al., 2017)
Tuoji	38.19, 120.74	AE21	2014.12−2015.01	8 (532)	
Yulin	38.33, 109.72	PSAP	2001.03−05	6	(Xu, 2004)

Photoacoustic Extinctiometers, Boulder, PAX

Absorption Photometer, Radiance Research, PSAP

Table S3 Differences of meteorological conditions (temperature (T), relative humidity (RH), pressure (P), visibility (Vis), and boundary layer height (BLH)) at the five observation sites.

		HA	LH	SX	WH
T	LH				
	SX				
	WH				
	XY				
RH	LH				
	SX				
	WH				
	XY				
P	LH				
	SX				
	WH				
	XY				
Vis	LH				
	SX				
	WH				
	XY				
BLH	LH				
	SX				
	WH				
	XY				

Pink color means that the difference between the two variables was significant at 0.05 level; yellow color means that the difference between two variables was not significant.

Table S4 Number of data for the different air quality in Figure 4.

	HA	LH	SX	WH	XY
Clean	17424	7629	10500	1983	2315
Light pollution	7650	14303	9720	1632	13334
Heavy pollution	/	2313	/	/	2856

/: no heavy pollution episode existed.

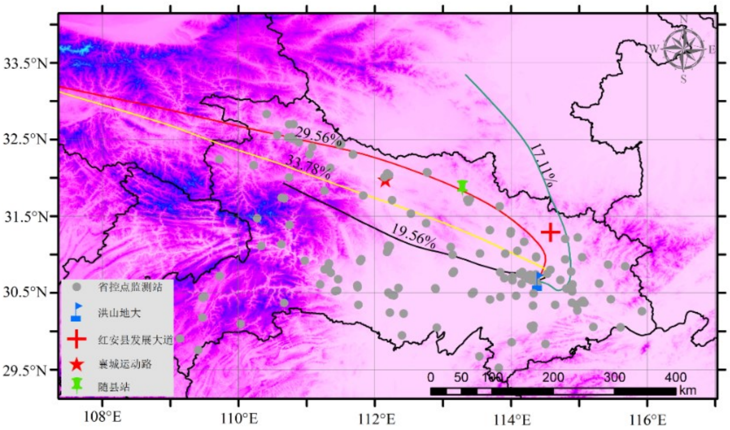

Figure S1 Cluster analysis results of air masses transported to Wuhan in January 2017.

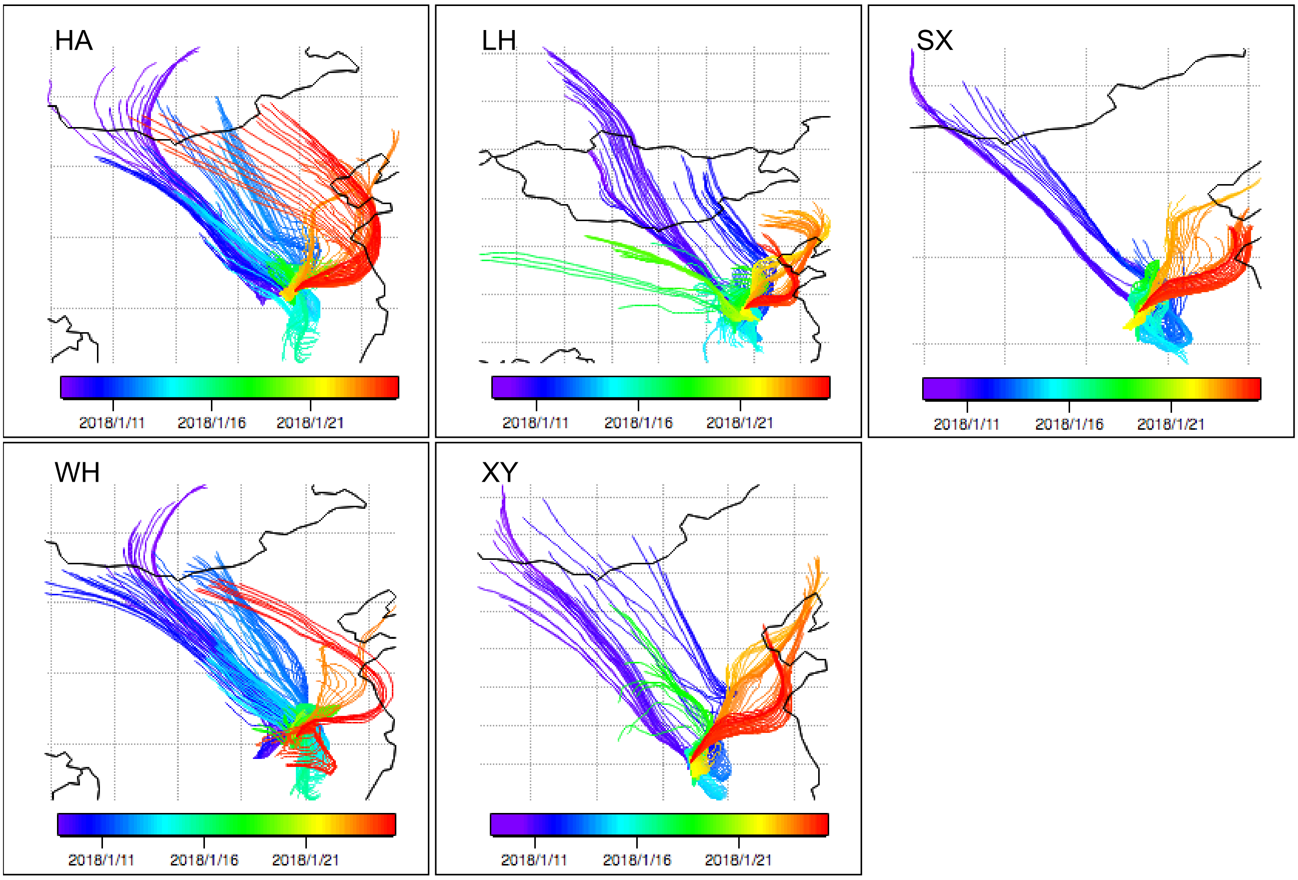

Figure S2 Hourly trajectories reaching at the five sites during the observation period.

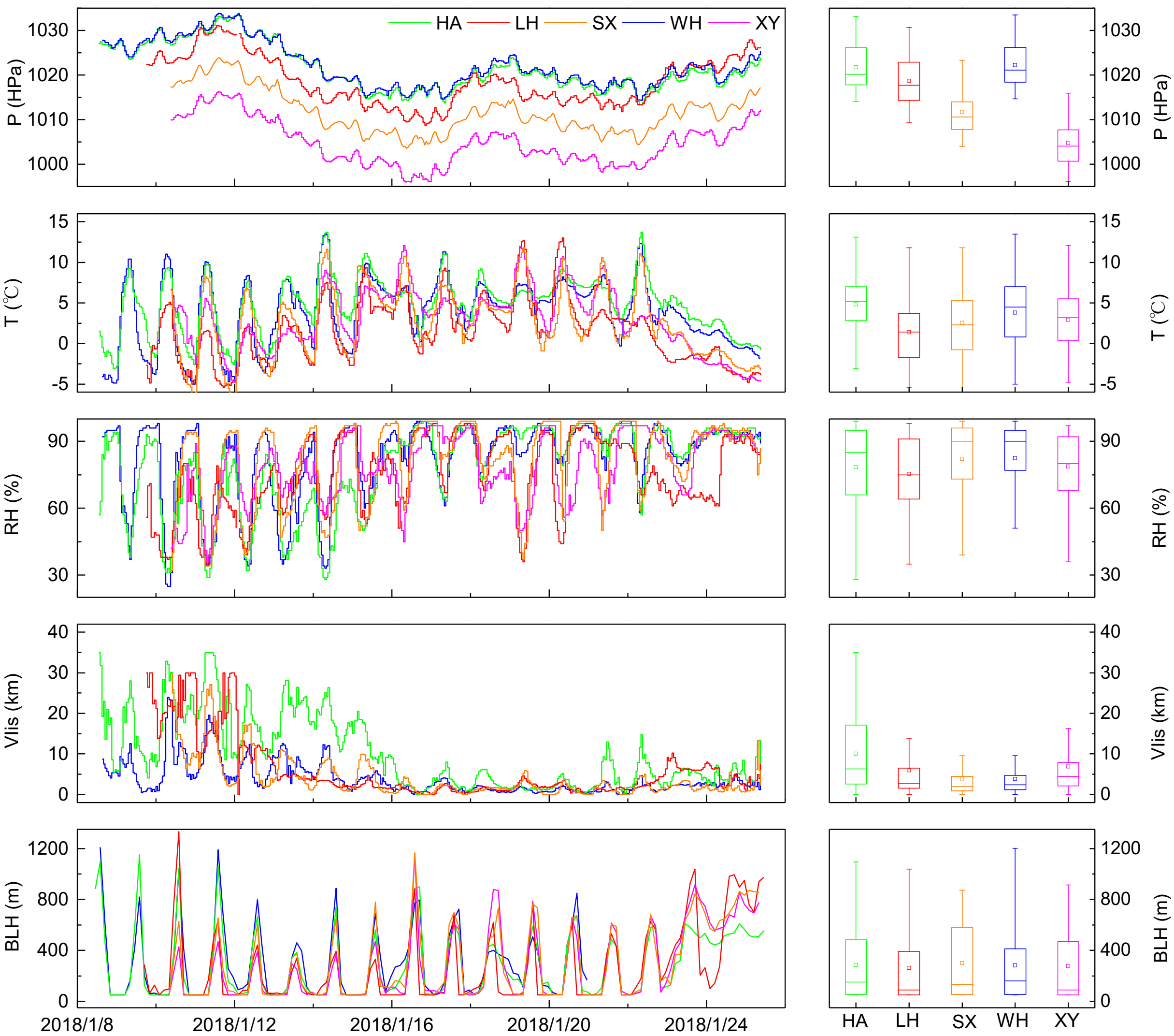

Figure S3 Time series and box plots of meteorological parameters including pressure (P), temperature (T), relative humidity (RH), visibility (Vis), and boundary layer height (BLH) at the five sites.

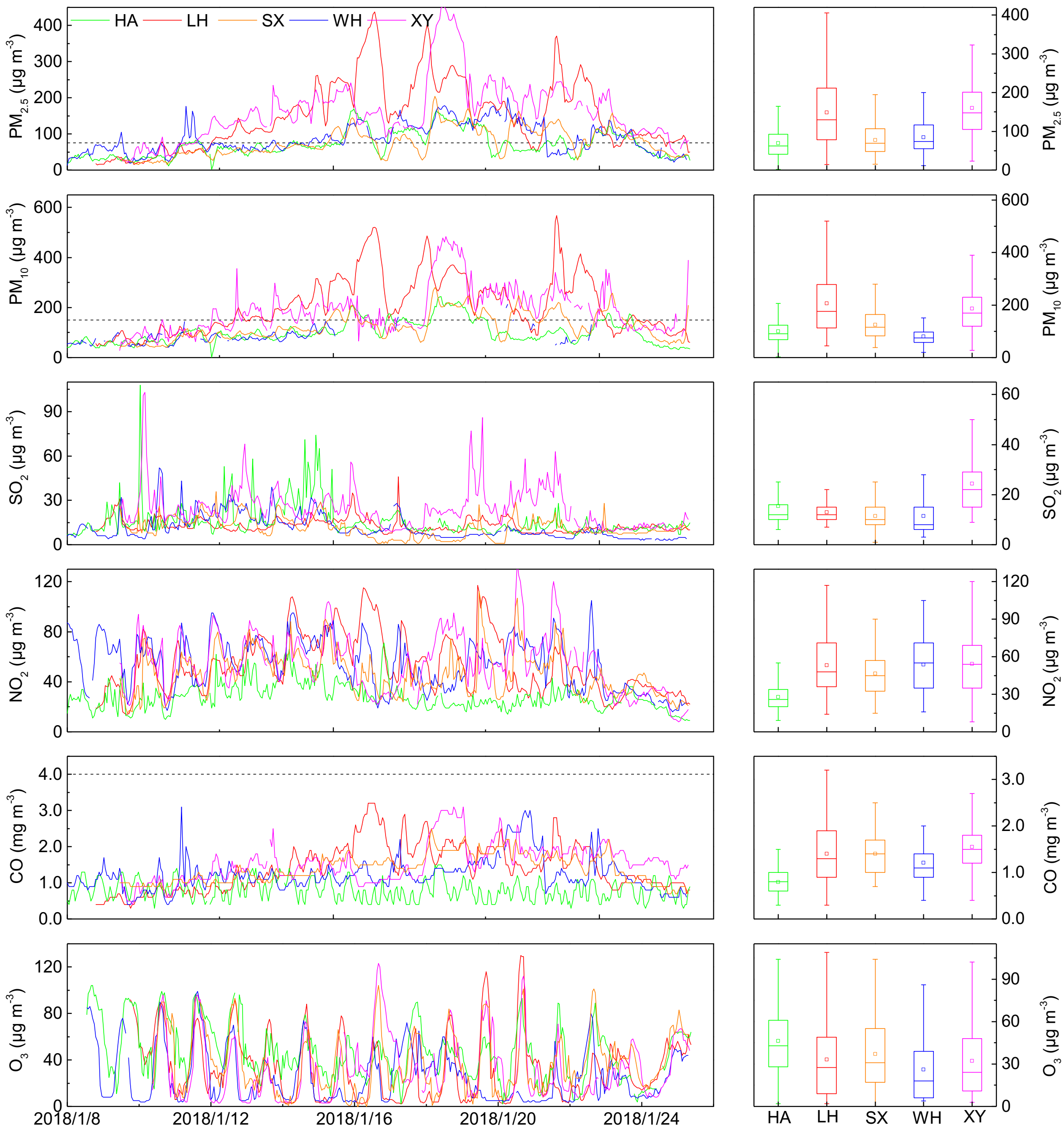

Figure S4 Time series and box plots of the hourly averaged $PM_{2.5}$, PM_{10}, SO_2, NO_2, CO, and O_3 concentrations at the five sites for the observation period (2018/1/8~2018/1/25). The dash lines are the corresponding daily secondary standards of the ambient air quality in China (GB3095−2012). The SO_2, CO and O_3 concentrations were lower than their secondary standards (150 μg m^{-3} for SO_2, 4 mg m^{-3} for CO, and 160 μg m^{-3} for O_3) during the entire periods.

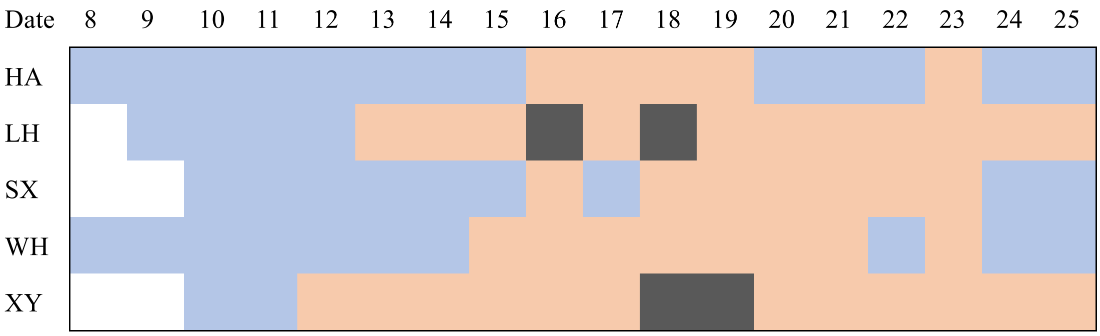

Figure S5 Daily air quality of each site during the observation periods. The blue, orange and dark stand for good ($PM_{2.5}$ < 75 μg m^{-3}), light polluted (75 < $PM_{2.5}$ < 250 μg m^{-3}) and heavily polluted ($PM_{2.5}$ > 250 μg m^{-3}) air quality, respectively.

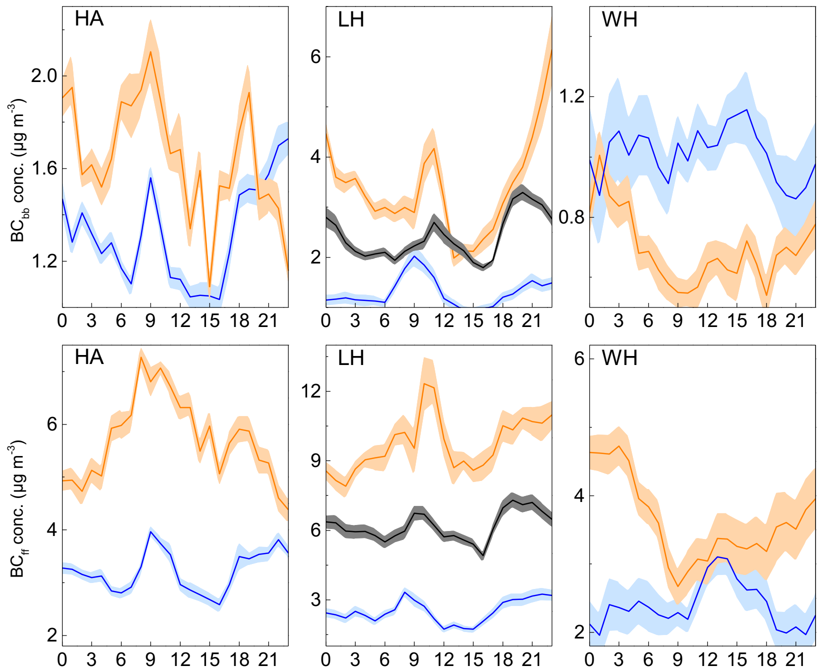

Figure S6 Diurnal variations of BC$_{bb}$ (up panel) and BC$_{ff}$ (bottom panel) at HA, LH and WH under different air quality.

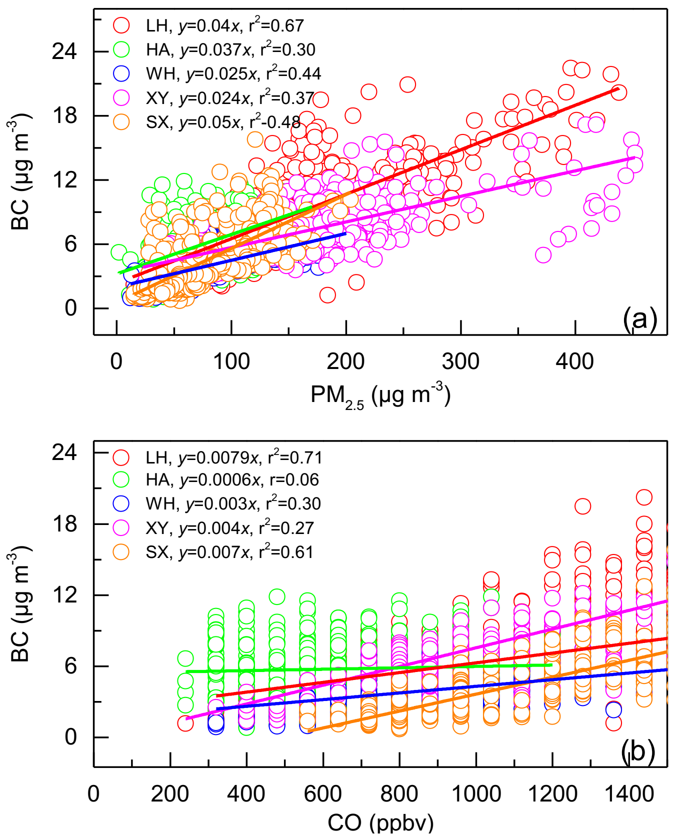

Figure S7 Scatter plots of BC vs $PM_{2.5}$ (a) and BC vs CO (b).

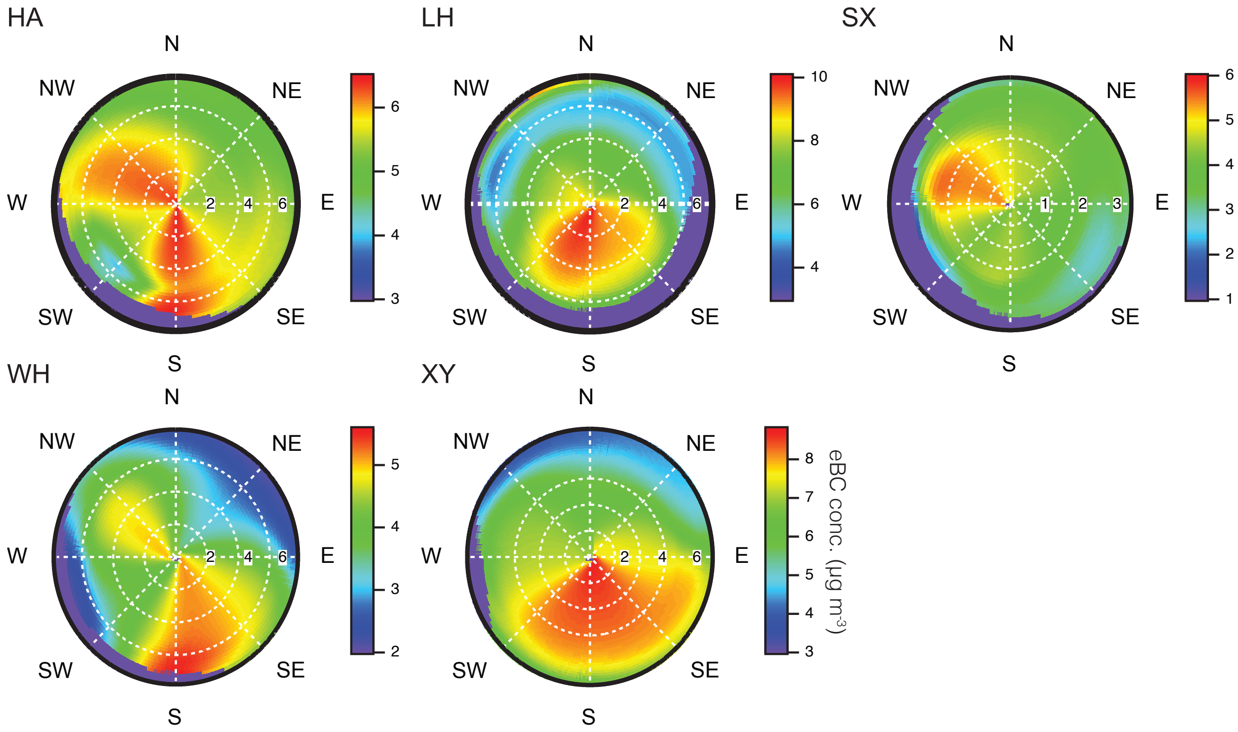

Figure S8 Nonparametric wind regression (NWR) plots of eBC at the five observation sites.

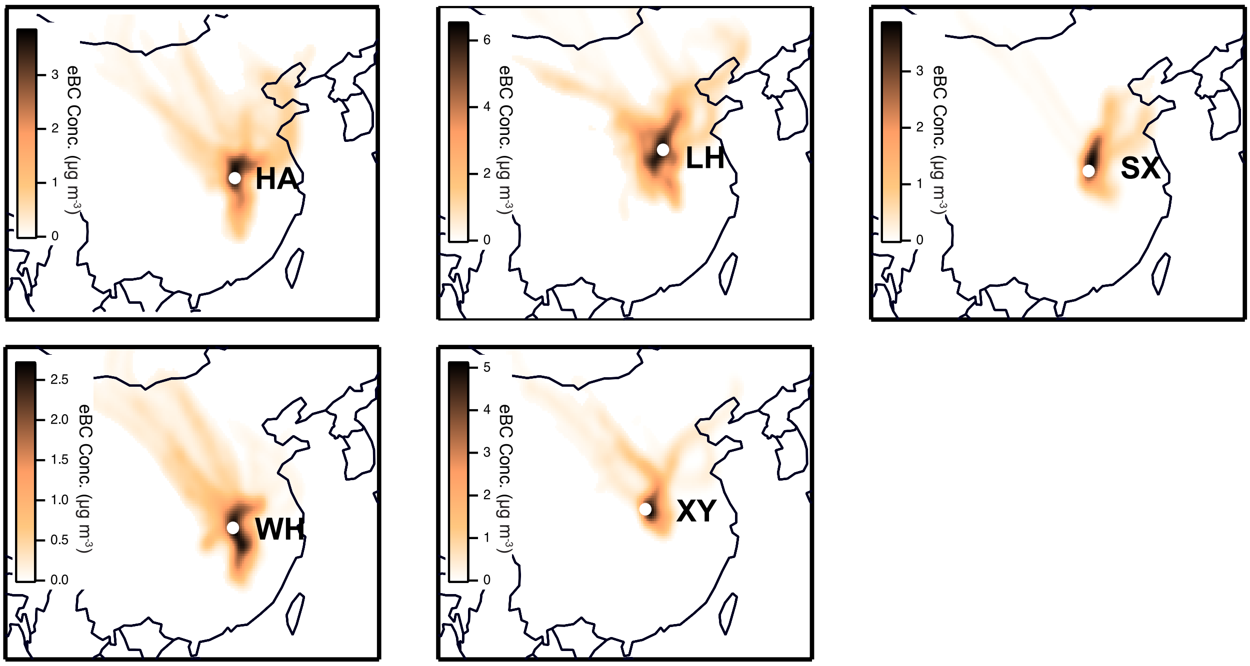

Figure S9 CWT results of eBC at the five sites during the observation period

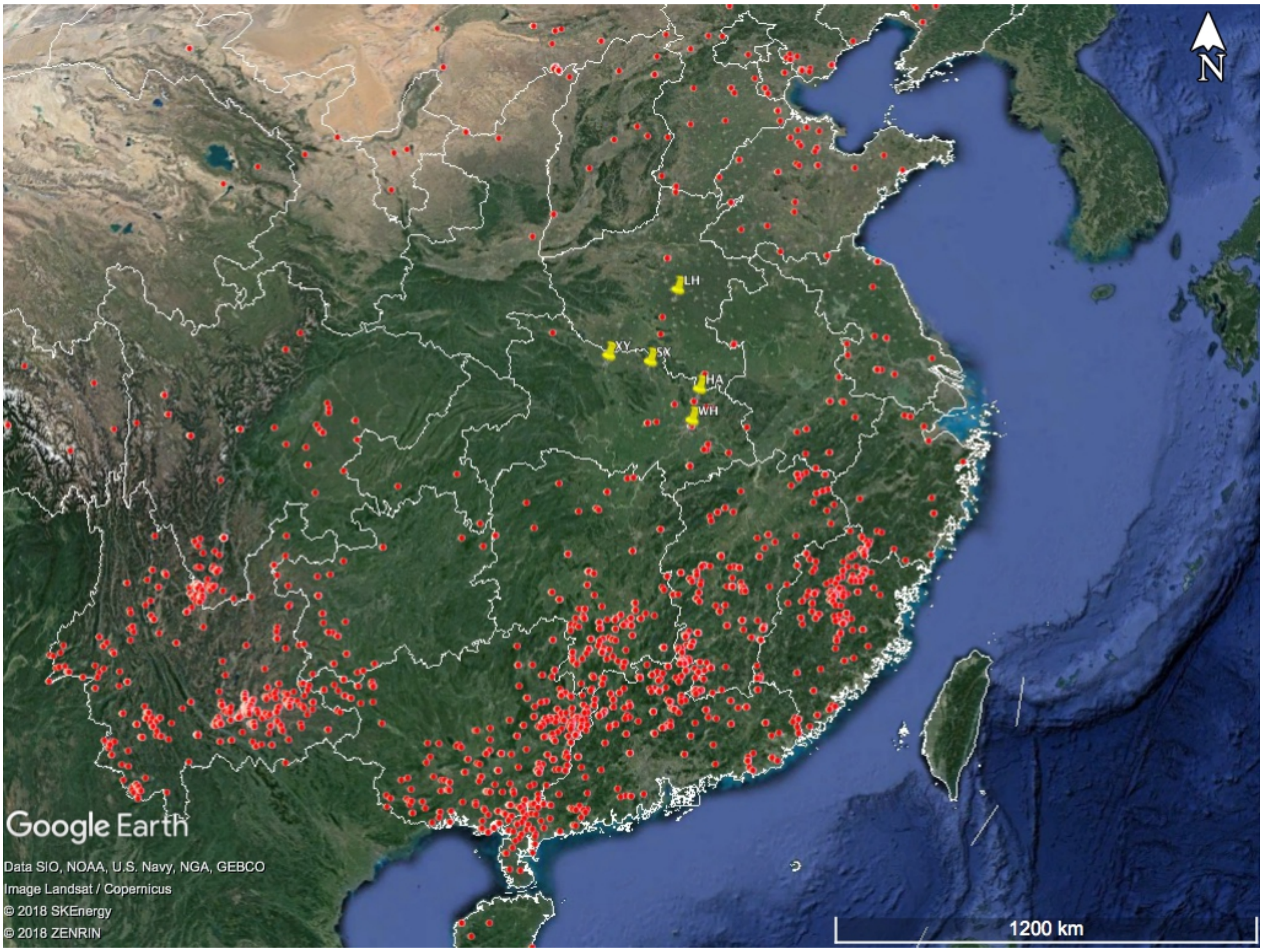

Figure S10 Locations of the fire spots downloaded from MODIS during the observation period (2018/1/08~2018/1/25).

Reference

Cheng, T., Xu, C., Duan, J., Wang, Y., Leng, C., Tao, J., Che, H., He, Q., Wu, Y., Zhang, R., Li, X., Chen, J., Kong, L. and Yu, X.: Seasonal variation and difference of aerosol optical properties in columnar and surface atmospheres over Shanghai, Atmos. Environ., 123, 315–326, doi:10.1016/j.atmosenv.2015.05.029, 2015.

Cheng, Y. F., Wiedensohler, A., Eichler, H., Su, H., Gnauk, T., Brüggemann, E., Herrmann, H., Heintzenberg, J., Slanina, J. and Tuch, T.: Aerosol optical properties and related chemical apportionment at Xinken in Pearl River Delta of China, Atmos. Environ., 42(25), 6351–6372, doi:10.1016/j.atmosenv.2008.02.034, 2008.

Chiloane, K. E., Beukes, J. P., van Zyl, P. G., Maritz, P., Vakkari, V., Josipovic, M., Venter, A. D., Jaars, K., Tiitta, P., Kulmala, M., Wiedensohler, A., Liousse, C., Mkhatshwa, G. V., Ramandh, A. and Laakso, L.: Spatial, temporal and source contribution assessments of black carbon over the northern interior of South Africa, Atmos. Chem. Phys., 17(10), 6177–6196, doi:10.5194/acp-17-6177-2017, 2017.

Deng, J., Zhang, Y., Hong, Y., Xu, L., Chen, Y., Du, W. and Chen, J.: Optical properties of PM 2.5 and the impacts of chemical compositions in the coastal city Xiamen in China, Sci. Total Environ., 557–558, 665–675, doi:10.1016/j.scitotenv.2016.03.143, 2016.

Fan, X., Chen, H., Xia, X., Li, Z. and Cribb, M.: Aerosol optical properties from the Atmospheric Radiation Measurement Mobile Facility at Shouxian, China, J. Geophys. Res., 115, doi:10.1029/2010JD014650, 2010.

Gao, C., Zhang, R. and Su, L.: Characteristic analysis of atmospheric black carbon aerosols in Changchun in autumn and winter, Plateau Meteorol., 28(4), 803–807, 2009.

Garland, R. M., Yang, H., Schmid, O., Rose, D., Nowak, A., Achtert, P., Wiedensohler, A., Takegawa, N., Kita, K., Miyazaki, Y., Kondo, Y., Hu, M., Shao, M., Zeng, L. M., Zhang, Y. H., Andreae, M. O. and Pöschl, U.: Aerosol optical properties in a rural environment near the mega-city Guangzhou, China: implications for regional air pollution, radiative forcing and remote sensing,Atmos. Chem. Phys., 8(17), 5161–5186, doi:10.5194/acp-8-5161-2008, 2008.

Garland, R. M., Schmid, O., Nowak, A., Achtert, P., Wiedensohler, A., Gunthe, S. S., Takegawa, N., Kita, K., Kondo, Y., Hu, M., Shao, M., Zeng, L. M., Zhu, T., Andreae, M. O. and Pöschl, U.: Aerosol optical properties observed during Campaign of Air Quality Research in Beijing 2006 (CAREBeijing-2006): Characteristic differences between the inflow and outflow of Beijing city air, J. Geophys. Res., 114, doi:10.1029/2008JD010780, 2009.

He, X., Li, C. C., Lau, A. K. H., Deng, Z. Z., Mao, J. T., Wang, M. H. and Liu, X. Y.: An intensive study of aerosol optical properties in Beijing urban area, Atmos. Chem. Phys., 9(22), 8903–8915, doi:10.5194/acp-9-8903-2009, 2009.

Healy, R. M., Sofowote, U., Su, Y., Debosz, J., Noble, M., Jeong, C.H., Wang, J. M., Hilker, N., Evans, G. J., Doerksen, G., Jones, K. and Munoz, A.: Ambient measurements and source apportionment of fossil fuel and biomass burning black carbon in Ontario, Atmos. Environ., 161, 34–47, doi:10.1016/j.atmosenv.2017.04.034, 2017.

Huang, X.F., Sun, T.L., Zeng, L.W., Yu, G.H. and Luan, S.J.: Black carbon aerosol characterization in a coastal city in South China using a single particle soot photometer, Atmos. Environ., 51, 21–28, doi:10.1016/j.atmosenv.2012.01.056, 2012.

Huang, X.F., Xue, L., Tian, X.-D., Shao, W.-W., Sun, T.L., Gong, Z.H., Ju, W.W., Jiang, B., Hu, M. and He, L.Y.: Highly time-resolved carbonaceous aerosol characterization in Yangtze River Delta of China: Composition, mixing state and secondary formation, Atmos. Environ., 64, 200–207, doi:10.1016/j.atmosenv.2012.09.059, 2013.

Hyvärinen, A.P., Kolmonen, P., Kerminen, V.M., Virkkula, A., Leskinen, A., Komppula, M., Hatakka, J., Burkhart, J., Stohl, A., Aalto, P., Kulmala, M., Lehtinen, K. E. J., Viisanen, Y. and Lihavainen, H.: Aerosol black carbon at five background measurement sites over Finland, a gateway to the Arctic, Atmos. Environ., 45(24), 4042–4050, doi:10.1016/j.atmosenv.2011.04.026, 2011.

Ji, D., Li, L., Pang, B., Xue, P., Wang, L., Wu, Y., Zhang, H. and Wang, Y.: Characterization of black carbon in an urban-rural fringe area of Beijing, Environ. Pollut., 223, 524–534, doi:10.1016/j.envpol.2017.01.055, 2017.

Li, C., Marufu, L. T., Dickerson, R. R., Li, Z., Wen, T., Wang, Y., Wang, P., Chen, H. and Stehr, J. W.: In situ measurements of trace gases and aerosol optical properties at a rural site in northern China during East Asian Study of Tropospheric Aerosols: An International Regional Experiment 2005, J. Geophys. Res., 112(D22), doi:10.1029/2006JD007592, 2007.

Lin, C. Q., Liu, G., Lau, A. K. H., Li, Y., Li, C. C., Fung, J. C. H. and Lao, X. Q.: High-resolution satellite remote sensing of provincial PM 2.5 trends in China from 2001 to 2015, Atmos. Environ., 180, 110–116, doi:10.1016/j.atmosenv.2018.02.045, 2018.

Liu, Q., Ma, T., Olson, M. R., Liu, Y., Zhang, T., Wu, Y. and Schauer, J. J.: Temporal variations of black carbon during haze and non-haze days in Beijing, Sci. Rep., 6(1), doi:10.1038/srep33331, 2016.

Ma, N., Zhao, C. S., Nowak, A., Müller, T., Pfeifer, S., Cheng, Y. F., Deng, Z. Z., Liu, P. F., Xu, W. Y., Ran, L., Yan, P., Göbel, T., Hallbauer, E., Mildenberger, K., Henning, S., Yu, J., Chen, L. L., Zhou, X. J., Stratmann, F. and Wiedensohler, A.: Aerosol optical properties in the North China Plain during HaChi campaign: an in-situ optical closure study, Atmos. Chem. Phys., 11(12), 5959–5973, doi:10.5194/acp-11-5959-2011, 2011.

Petit, J.E., Amodeo, T., Meleux, F., Bessagnet, B., Menut, L., Grenier, D., Pellan, Y., Ockler, A., Rocq, B., Gros, V., Sciare, J. and Favez, O.: Characterising an intense PM pollution episode in March 2015 in France from multi-site approach and near real time data: Climatology, variabilities, geographical origins and model evaluation, Atmos. Environ., 155, 68–84, doi:10.1016/j.atmosenv.2017.02.012, 2017.

Shen, Y., Virkkula, A., Ding, A., Wang, J., Chi, X., Nie, W., Qi, X., Huang, X., Liu, Q., Zheng, L., Xu, Z., Petäjä, T., Aalto, P. P., Fu, C. and Kulmala, M.: Aerosol Optical Properties at SORPES in Nanjing, East China, Atmos. Chem. Phys. Discuss., 1–46, doi:10.5194/acp-2017-863, 2017.

Tan, H., Liu, L., Fan, S., Li, F., Yin, Y., Cai, M. and Chan, P. W.: Aerosol optical properties and mixing state of black carbon in the Pearl River Delta, China, Atmos. Environ., 131, 196–208, doi:10.1016/j.atmosenv.2016.02.003, 2016.

Tao, J., Zhang, L., Cao, J. and Zhang, R.: A review of current knowledge concerning $PM_{2.5}$: chemical composition, aerosol optical properties and their relationships across China, Atmos. Chem. Phys., 17(15), 9485–9518, doi:10.5194/acp-17-9485-2017, 2017.

Wan, X., Kang, S., Wang, Y., Xin, J., Liu, B., Guo, Y., Wen, T., Zhang, G. and Cong, Z.: Size distribution of carbonaceous aerosols at a high-altitude site on the central Tibetan Plateau (Nam Co Station, 4730ma.s.l.), Atmos. Res., 153, 155–164, doi:10.1016/j.atmosres.2014.08.008, 2015.

Wang, H., He, Q., Chen, Y. and Kang, Y.: Characterization of black carbon concentrations of haze with different intensities in Shanghai by a three-year field measurement, Atmos. Environ., 99, 536–545, doi:10.1016/j.atmosenv.2014.10.025, 2014a.

Wang, H., Shi, G., Tian, M., Zhang, L., Chen, Y., Yang, F. and Cao, X.: Aerosol optical properties and chemical composition apportionment in Sichuan Basin, China, Sci. Total Environ., 577, 245–257, doi:10.1016/j.scitotenv.2016.10.173, 2017a.

Wang, J., Virkkula, A., Gao, Y., Lee, S., Shen, Y., Chi, X., Nie, W., Liu, Q., Xu, Z., Huang, X., Wang, T., Cui, L. and Ding, A.: Observations of aerosol optical properties at a coastal site in Hong Kong, South China, Atmos. Chem. Phys., 17(4), 2653–2671, doi:10.5194/acp-17-2653-2017, 2017b.

Wang, M., Xu, B., Wang, N., Cao, J., Tie, X., Wang, H., Zhu, C. and Yang, W.: Two distinct patterns of seasonal variation of airborne black carbon over Tibetan Plateau, Sci. Total Environ., 573, 1041–1052, doi:10.1016/j.scitotenv.2016.08.184, 2016.

Wang, Q., Huang, R.J., Cao, J., Han, Y., Wang, G., Li, G., Wang, Y., Dai, W., Zhang, R. and Zhou, Y.: Mixing State of Black Carbon Aerosol in a Heavily Polluted Urban Area of China: Implications for Light Absorption Enhancement, Aerosol Sci. Technol., 48(7), 689–697, doi:10.1080/02786826.2014.917758, 2014b.

Wang, Q., Cao, J., Han, Y., Tian, J., Zhu, C., Zhang, Y., Zhang, N., Shen, Z., Ni, H., Zhao, S. and Wu, J.: Sources and physicochemical characteristics of black carbon aerosol from the southeastern Tibetan Plateau: internal mixing enhances light absorption, Atmos. Chem. Phys., 18(7), 4639–4656, doi:10.5194/acp-18-4639-2018, 2018.

Wang, Q. Y., Huang, R.-J., Cao, J. J., Tie, X. X., Ni, H. Y., Zhou, Y. Q., Han, Y. M., Hu, T. F., Zhu, C. S., Feng, T., Li, N. and Li, J. D.: Black carbon aerosol in winter northeastern Qinghai–Tibetan Plateau, China: the source, mixing state and optical property, Atmos. Chem. Phys., 15(22), 13059–13069, doi:10.5194/acp-15-13059-2015, 2015.

Wang, Y., Ma, Y., Lu, Z., Zhou, D., Liu, N., Zhang, Y. and Hong, Y.: In Situ Continuous Observation of Atmospheric Black Carbon Aerosol Mass Concentration in Liaoning Region, Res. Environ. Sci., 24(10), 1088–1096, 2011.

Weingartner, E., Saathoff, H., Schnaiter, M., Streit, N., Bitnar, B. and Baltensperger, U.: Absorption of light by soot particles: determination of the absorption coefficient by means of aethalometers, J. Aerosol Sci., 34(10), 1445–1463, doi:10.1016/S0021-8502(03)00359-8, 2003.

Wu, D., Mao, J., Deng, X., Tie, X., Zhang, Y., Zeng, L., Li, F., Tan, H., Bi, X., Huang, X., Chen, J. and Deng, T.: Black carbon aerosols and their radiative properties in the Pearl River Delta region, Sci. China Ser. Earth Sci., 52(8), 1152–

1163, doi:10.1007/s11430-009-0115-y, 2009.

Wu, D., Wu, C., Liao, B., Chen, H., Wu, M., Li, F., Tan, H., Deng, T., Li, H., Jiang, D. and Yu, J. Z.: Black carbon over the South China Sea and in various continental locations in South China, Atmos. Chem. Phys., 13(24), 12257–12270, doi:10.5194/acp-13-12257-2013, 2013.

Wu, Y.: Aerosol Optical Properties Observed at a Semi-arid Rural Site in Northeastern China, Aerosol Air Qual. Res., doi:10.4209/aaqr.2011.11.0202, 2012.

Wu, Y., Zhang, R., Tian, P., Tao, J., Hsu, S.-C., Yan, P., Wang, Q., Cao, J., Zhang, X. and Xia, X.: Effect of ambient humidity on the light absorption amplification of black carbon in Beijing during January 2013, Atmos. Environ., 124, 217–223, doi:10.1016/j.atmosenv.2015.04.041, 2016.

Xu, J.: Aerosol chemical, physical, and radiative characteristics near a desert source region of northwest China during ACE-Asia, J. Geophys. Res., 109(D19), doi:10.1029/2003JD004239, 2004.

Xu, J., Bergin, M. H., Yu, X., Liu, G., Zhao, J., Carrico, C. M. and Baumann, K.: Measurement of aerosol chemical, physical and radiative properties in the Yangtze delta region of China, Atmos. Environ., 36(2), 161–173, doi:10.1016/S1352-2310(01)00455-1, 2002.

Xu, J., Tao, J., Zhang, R., Cheng, T., Leng, C., Chen, J., Huang, G., Li, X. and Zhu, Z.: Measurements of surface aerosol optical properties in winter of Shanghai, Atmos. Res., 109–110, 25–35, doi:10.1016/j.atmosres.2012.02.008, 2012.

Yan, P., Tang, J., Huang, J., Mao, J. T., Zhou, X. J., Liu, Q., Wang, Z. F. and Zhou, H. G.: The measurement of aerosol optical properties at a rural site in Northern China, Atmos. Chem Phys, 14, 2008.

Yan, W., Yang, L., Chen, J., Wang, X., Wen, L., Zhao, T. and Wang, W.: Aerosol optical properties at urban and coastal sites in Shandong Province, Northern China, Atmos. Res., 188, 39–47, doi:10.1016/j.atmosres.2016.12.011, 2017.

Yu, X., Ma, J., Raghavendra Kumar, K., Zhu, B., An, J., He, J. and Li, M.: Measurement and analysis of surface aerosol optical properties over urban Nanjing in the Chinese Yangtze River Delta, Sci. Total Environ., 542, 277–291, doi:10.1016/j.scitotenv.2015.10.079, 2016.

Zhang, L., Zhang, L., Zhang, D., Zhao, S., Huang, J., Zhang, W. and Shi, J.: Property of black carbon concentration over outskirts of Lanzhou, Northwest China, China Environ. Sci., 31(8), 1248–1255, 2011.

Zhang, X. Y., Wang, Y. Q., Niu, T., Zhang, X. C., Gong, S. L., Zhang, Y. M. and Sun, J. Y.: Atmospheric aerosol compositions in China: spatial/temporal variability, chemical signature, regional haze distribution and comparisons with global aerosols,Atmos. Chem. Phys., 12(2), 779–799, doi:10.5194/acp-12-779-2012, 2012.

Zhu, C.S., Cao, J.J., Ho, K.F., Antony Chen, L.W., Huang, R.J., Wang, Y.C., Li, H., Shen, Z.X., Chow, J. C., Watson, J. G., Su, X., Wang, Q. and Xiao, S.: The optical properties of urban aerosol in northern China: A case study at Xi'an,Atmos. Res., 160, 59–67, doi:10.1016/j.atmosres.2015.03.008, 2015.

Zhu, C.S., Cao, J.J., Xu, B.Q., Huang, R.J., Wang, P., Ho, K.F., Shen, Z.X., Liu, S.X., Han, Y.M., Tie, X.X., Zhao, Z.Z. and Chen, L.W. A.: Black Carbon Aerosols at Mt. Muztagh Ata, a High-Altitude Location in the Western Tibetan

Plateau, Aerosol Air Qual. Res., 16(3), 752–763, doi:10.4209/aaqr.2015.04.0255, 2016.

Zhu, C.S., Cao, J.J., Hu, T.F., Shen, Z.X., Tie, X.X., Huang, H., Wang, Q.Y., Huang, R.J., Zhao, Z.Z., Močnik, G. and Hansen, A. D. A.: Spectral dependence of aerosol light absorption at an urban and a remote site over the Tibetan Plateau, Sci. Total Environ., 590–591, 14–21, doi:10.1016/j.scitotenv.2017.03.057, 2017.

Zhuang, B., Wang, T., Liu, J., Li, S., Xie, M., Han, Y., Chen, P., Hu, Q., Yang, X., Fu, C. and Zhu, J.: The surface aerosol optical properties in the urban area of Nanjing, west Yangtze River Delta, China, Atmos. Chem. Phys., 17(2), 1143–1160, doi:10.5194/acp-17-1143-2017, 2017.

Zhuang, B. L., Wang, T. J., Liu, J., Li, S., Xie, M., Yang, X. Q., Fu, C. B., Sun, J. N., Yin, C. Q., Liao, J. B., Zhu, J. L. and Zhang, Y.: Continuous measurement of black carbon aerosol in urban Nanjing of Yangtze River Delta, China, Atmos. Environ., 89, 415–424, doi:10.1016/j.atmosenv.2014.02.052, 2014.